Johann Radon Institute for
Computational and Applied Mathematics
Austrian Academy of Sciences (ÖAW)

Boundary control of a Bernoulli free boundary problem

H. Kasumba

RICAM-Report 2014-03

BOUNDARY CONTROL OF A BERNOULLI FREE BOUNDARY PROBLEM

H. KASUMBA

ABSTRACT. We present a boundary optimal control approach for a Bernoulli free boundary problem. Our control objective consists in tracking a free boundary to an a priori given desired one. An appropriate cost functional is chosen for this purpose and its gradient is analytically derived. The resulting optimality conditions are discretized and the minimization problem is solved numerically by a steepest descent method. Numerical simulations show the applicability of the proposed method.

1. INTRODUCTION

An optimal control of a partial differential equation (PDE) involve varying an input control function such that the resultant state y (determined a solution to a PDE), has some desirable property. This desired property is measured according to some functional J, called the objective functional.

Usually, the partial differential equation is formulated and solved in known domains, (see for instance the monographs [16, 21, 31] and references there in). If the state y is defined by a free boundary problem, the situation becomes more involved. Specifically, the function y and the domain Ω where the PDE is considered are now unknown, and they have to be found simultaneously as part of the solution of the direct (forward) problem. Furthermore, one has to account for the variation of the domain in the derivation of the sensitivity equations.

Control of problems defined on unknown domains play a crucial role in the quality assessment of many applications such as continuous casting of steel [23], welding processes [33], thin film manufacturing processes [26], to mention but a few.

There have been various attempts to solve optimal control problems with a free boundary problem as a constraint. In [17, 18], the authors study the optimal control of a two phase Stefan problem where the free boundary is modeled using a graph. In [3], the same problem is considered where the interface is implicitly parametrized using a level set function. In [25], the authors consider an optimal control of a free-surface flow governed by Stokes equation, where the interface is explicitly parametrized using graphs. Explicit parametrization is a more natural way to describe interfaces in free surface flows [24]. However, the description of an interface or free boundary using graphs is restrictive and can only be applied on specific geometries. Therefore, in this work, we consider an optimal control of a free surface

Key words and phrases. Optimal control, Bernoulli free boundary problem, Cost functional.

flow in a bounded domain of class $C^{1,\alpha}$, where the interface is explicitly parametrized using the position of nodes at the interface. We assume that the stationary regime has been reached and that the fluid is irrotational. Consequently, the description of free boundaries gives rise to the exterior Bernoulli free boundary problem [9, Pg. 138-140]. The exterior Bernoulli free boundary problem (BFP) can be stated as follows:
Given a bounded Lipschitz domain $\omega \subset \mathbb{R}^2$ with boundary Σ and a fixed function $\mu < 0$, find a bounded domain $\Omega \in \mathscr{O}_{ad}$ with a $C^{1,1}$ boundary Γ and a function y defined on $S := \Omega \setminus \bar{\omega}$ such that

$$-\Delta y = 0 \quad \text{in} \quad S, \tag{1}$$

$$y = 1 \quad \text{on} \quad \Sigma, \tag{2}$$

$$y = 0 \quad \text{on} \quad \Gamma, \tag{3}$$

$$\partial_{\mathbf{n}} y = \mu \quad \text{on} \quad \Gamma, \tag{4}$$

where

$$\mathscr{O}_{ad} = \{\Omega \subset \mathbb{R}^2 \text{ a bounded domain}: \ \overline{\omega} \subset \Omega, \ \overline{\Omega} \subset \mathscr{D}\}.$$

Here, $\mathbf{n}$ stands for the unit normal vector on the free boundary Γ and $\partial_{\mathbf{n}} y$ denotes the normal derivative of y. The geometric setup of (1)-(4) is depicted in Figure 1. Other applications

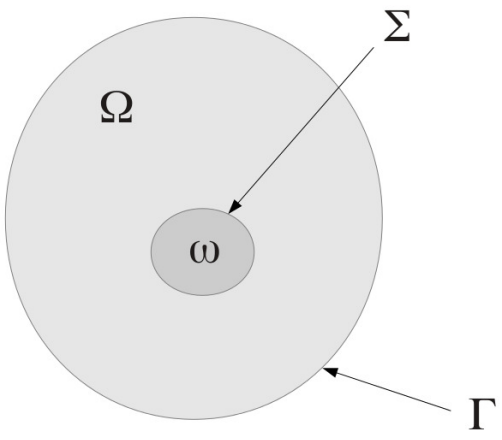

FIGURE 1. The exterior Bernoulli problem

leading to formulations like (1)-(4) include electrochemistry and electromagnetics [11]. A number of authors have analyzed and solved problem (1)-(4) for a given fixed domain ω, see for instance [9, Ch. 3], [2, 4, 5, 10, 11, 19, 22] and references therein. In this work, we are interested in obtaining a-priori given properties of Γ via optimization techniques. Recently, the authors in [29, 30] utilized the shape of ω as a control to drive the domain Ω as close

as possible to a given desired one, by minimizing appropriate cost functionals. On the other hand, if the domain ω is fixed, then for different values of the parameter $\mu < 0$, one obtains different locations of the free boundary Γ [10]. Therefore, to achieve our fore mentioned goal, the parameter μ in (4) is utilized as a control to drive the domain Ω as close as possible to a given desired one. This gives rise to an optimal control problem, where (1)-(4) represents the state constraint and μ the control. The state constraint itself can be formulated as an optimization; this approach has been used in [10, 19] for instance. Subsequently, we deal with a bilevel optimization problem [6, 7], where the constraint (1)-(4) constitutes the lower-level optimization problem, and the upper-level consists in minimization with respect to μ.

Turning to numerical realization of the bilevel optimization problem, two possible approaches exist, namely, either treating (μ,Ω) as controls and y as state or μ as control and (y,Ω) as states. Using the former strategy, solving for the state y becomes a classical linear boundary value problem with well-posed boundary data in the lower level problem. Unfortunately, as noted in [29], this approach leads to serious convergence problems. A further disadvantage that was noted in [29] is that, depending on the formulation, a locally optimal pair (y,Ω) might not represent a physical solution to the free boundary problem. For this reason, we adopt a latter approach, i.e., we find a solution to the free boundary problem first and then proceed to the upper level represented by the minimization of the cost functional.

Before we close this section, we collect some notations and definitions that we need in our subsequent discussion. We use bold fonts for vectors $\mathbf{x} = (x_1, x_2)^T \in \mathbb{R}^2$ with norm $|\mathbf{x}|_{\mathbb{R}^2} = (\sum_{j=1}^{2} x_j^2)^{1/2}$ and vector-valued functions are also indicated by bold letters. The unit outward normal and tangential vectors to a domain Ω shall be denoted by $\mathbf{n} = (n_1, n_2)$ and $\boldsymbol{\tau} = (-n_2, n_1)$, respectively. We denote by $W^{m,p}(\mathscr{S})$, $m \in \mathbb{N}$, $1 \le p \le \infty$ the standard L^p-Sobolev space of order m:

$$W^{m,p}(\mathscr{S}) := \left\{ u \in L^p(\mathscr{S}) \mid D^\beta u \in L^p(\mathscr{S}), \text{ for } 0 \le |\beta| \le m \right\},$$

where D^β is the weak (or distributional) partial derivative. Here $\mathscr{S}$ can be either $\mathbb{R}^2$, the flow domain Ω, its boundary $\partial\Omega$, or a subset of $\partial\Omega$. The norm $||\cdot||_{W^{m,p}(\mathscr{S})}$ associated with $W^{m,p}(\mathscr{S})$ is given by

$$||u||_{W^{m,p}(\mathscr{S})} = \left(\sum_{|\beta| \le m} \int_{\mathscr{S}} |D^\beta u|^p \, d\mathbf{x} \right)^{1/p}.$$

When $p = 2$ we write $H^m(\mathscr{S}) := W^{m,2}(\mathscr{S})$ for simplicity. The notation $|\Omega|$ denotes the Lebesgue measure of a set Ω and Ω^c its complementary. We write $\mathbb{1}_\Omega$ for the characteristic function of a set Ω, i.e.,

$$\mathbb{1}_\Omega(x) = \begin{cases} 1 & \text{if} \quad x \in \Omega, \\ 0 & \text{if} \quad x \notin \Omega. \end{cases} \tag{5}$$

The outline of the paper is as follows: In the next section, the well-posedness and numerical solution of the free boundary problem (1)-(4) is discussed. Thereafter, in Section 3, the optimization problem is introduced and the existence of the solution to this problem is briefly discussed. In Section 4, a sensitivity analysis of the optimization problem is performed, and the necessary optimality conditions are stated and proved. In section 5, a numerical algorithm for solving the optimal control problem is constructed and its performance is checked with help of 3 numerical examples. Possible extensions are addressed in the last section.

2. Well-posedness and numerical solution of the forward problem

2.1. **Well-posedness of the forward problem.** Let $\mathcal{V}_g := \{\varphi \in H^1(S) \ : \ \varphi = g \text{ on } \Sigma\}$. Then the weak formulation of (1)-(4) can be expressed as:
Find $(\Omega, y) \in \mathcal{O}_{ad} \times \mathcal{V}_1$ such that the following integral identities hold,

$$\int_S \nabla y \cdot \nabla \phi \, dx = \int_\Gamma \mu \phi \, ds \quad \text{for all} \quad \phi \in \mathcal{V}_0 \tag{6}$$

$$\int_\Gamma y \psi \, ds = 0 \quad \text{for all} \quad \psi \in L^2(\Gamma). \tag{7}$$

Here, $\mathcal{V}_0$ and $\mathcal{V}_1$ denote spaces with g replaced by 0 and 1, respectively, in $\mathcal{V}_g$.

Theorem 2.1. [1, 2] *If $\mu(x) \in H^1(\Gamma) < 0$ and Σ is a Lipschitz curve, then a solution to* (1)-(4) *or equivalently* (6)-(7) *exists and Γ is a $C^{1,\alpha}$ curve, for some $\alpha > 0$. Moreover, if the function $t \mapsto t\mu(x_0 + t(x - x_0))$ is decreasing in $t > 0$ for any $x \in \mathbb{R}^2$ and $x_0 \in \omega$, then Ω is unique. Furthermore, if $\mu_1(x)$, $\mu_2(x)$ are two Neumann fluxes and Γ_1, Γ_2, are the corresponding free boundaries in* (1)-(4)*, then $|\mu_1(x) - \mu_2(x)| \to 0$ implies that $\Delta(\Gamma_1, \Gamma_2) \to 0$, where*

$$\Delta(\Gamma_1, \Gamma_2) := \sup\{ln|\lambda| \ : \ \lambda\Gamma_1 \cap \Gamma_2 \neq \emptyset\}, \tag{8}$$

with $\lambda\Gamma := \{\lambda x \mid x \in \Gamma\}$.

2.2. **Numerical solution.** The numerical solution of the forward problem (1)-(4) can be achieved via two different strategies. First, an equivalent shape optimization problem can be considered and the corresponding cost functional minimized [10, 12, 19]; this requires the calculations of shape gradients that depends on known state and adjoint systems. Second, a fixed point type approach can be set up where a sequence of elliptic problems are solved in a sequence of converging domains, those domains being obtained through some updating rule based only on the solution of some state system at each iteration [11, 28]. Due to computational costs of the former scheme, namely, solution of two PDEs (state and adjoint) per iteration, we shall utilize a method that falls in the latter category. The structure of such a scheme is as follows:

(1) Choose an initial approximation of the free boundary Γ.
(2) Solve the boundary value problem (1)-(4) for y with one condition on Γ omitted.
(3) Update Γ using the discrepancy left by the remaining boundary condition.

(4) Iterate from step (2) until stationarity up to a specified accuracy is reached.

This scheme is simple to implement but it is not obvious how to construct the updating step in such a manner that the method converges and that the convergence is fast.

2.2.1. *Fixed point algorithm.* Before we derive the optimal updating step of a fixed point algorithm, we briefly recall some basic concepts and results related to shape differentiation [9, 27]. Assume that there is a fixed convex bounded set $\mathscr{D} \subset \mathbb{R}^2$ such that $\Omega \subset \bar{\mathscr{D}}$. Let

$$\mathscr{H} = \{\mathbf{V} \in C^{1,1}(\bar{\mathscr{D}}) : \mathbf{V} = 0 \text{ on } \partial D \cup \Sigma\}$$

be the space of deformation fields. Then the fields $\mathbf{V} \in \mathscr{H}$ define for $t > 0$, a perturbation of S by

$$\begin{aligned} T_t : S &\mapsto S_t, \\ \mathbf{x} &\mapsto T_t(\mathbf{x}) = \mathbf{x} + t\mathbf{V}(\mathbf{x}). \end{aligned}$$

For each $\mathbf{V} \in \mathscr{H}$, there exists $\tilde{\tau} > 0$ such that $T_t(\mathscr{D}) = \mathscr{D}$ and $\{T_t\}$ is a family of $C^{1,1}$- diffeomorphisms for $|t| < \tilde{\tau}$ [9]. For each $t \in \mathbb{R}$ with $|t| < \tilde{\tau}$, we set $S_t = T_t(S)$, $\Gamma_t = T_t(\Gamma)$. Thus $S_0 = S$, $\Gamma_0 = \Gamma$, $S_t \subset D$. For a given functional $\mathscr{J} : S \mapsto \mathbb{R}$, and a vector field $\mathbf{V} \in \mathscr{H}$, we say that $\mathscr{J}$ has a directional Eulerian shape derivative in direction $\mathbf{V}$ at S if the limit

$$d\mathscr{J}(S;\mathbf{V}) := \lim_{t \to 0^+} \frac{\mathscr{J}(S_t) - \mathscr{J}(S)}{t}. \tag{9}$$

exists. Furthermore, if $d\mathscr{J}(S;\mathbf{V})$ is linear and continuous with respect to $\mathbf{V}$, then we say that $\mathscr{J}$ is shape differentiable at S.

The second order shape derivative (Hessian) can be defined in an analogous manner. Specifically, let $\mathbf{V}$ and $\mathbf{W}$ be given vector fields in $\mathscr{H}$ and denote $S_t(\mathbf{W}) = T_t(\mathbf{W})(S)$ with $T_t(\mathbf{W})$ the transformation related to $\mathbf{W}$. If we assume that $d\mathscr{J}(S_t(\mathbf{W});\mathbf{V})$ exists for all $t \in I := [0, \tilde{\tau}]$, then we say that the functional $\mathscr{J}$ has a second order Eulerian semi-derivative at S in directions $(\mathbf{V}, \mathbf{W})$ if

$$d^2\mathscr{J}(S;\mathbf{V},\mathbf{W}) = \lim_{t \to 0^+} \frac{d\mathscr{J}(S_t(\mathbf{W});\mathbf{V}) - d\mathscr{J}(S;\mathbf{V})}{t}. \tag{10}$$

exists. Furthermore, if $d^2\mathscr{J}(S;\mathbf{V},\mathbf{W})$ is bilinear and continuous with respect to $(\mathbf{V},\mathbf{W}) \in \mathscr{H} \times \mathscr{H}$, then we say that $\mathscr{J}$ is twice shape differentiable at S.

An element $y' \in H^1(S)$ is called shape derivative of y at S in the direction $\mathbf{V}$ if the following limit exists in $H^1(S)$:

$$y'(\mathbf{x}) := \lim_{t \to 0^+} \frac{y_t(\mathbf{x}) - y(\mathbf{x})}{t}. \tag{11}$$

where $y_t(\mathbf{x})$ is defined in S_t. We are now in position to derive the optimal updating step for the fixed point algorithm to be precised later. To construct this algorithm, we follow the shape optimization approach first introduced by Tiihonen in [28] to solve problem (1)-(4) for a constant parameter μ. Here, $\mu = \mu(\mathbf{x})$ and hence the situation slightly changes, i.e.,

instead of robin boundary condition on Γ, we consider the following reformulation of the forward problem (1)-(4) as a shape optimization problem [19],

$$\min_{\Gamma} \quad \mathscr{J}(S) := \frac{1}{2}\int_{\Gamma} y^2 \, ds, \tag{12}$$

subject to

$$-\Delta y = 0 \quad \text{in} \quad S, \tag{13}$$

$$y = 1 \quad \text{on} \quad \Sigma, \tag{14}$$

$$\partial_{\mathbf{n}} y = \mu(\mathbf{x}) \quad \text{on} \quad \Gamma, \tag{15}$$

where the boundary ∂S is the disjoint union of a fixed part Σ and an unknown part Γ both being non-empty and such that $\text{dis}(\Sigma,\Gamma) > 0$. Note that a solution (y,Γ) of (1)-(4) provides a global minimizer for (12) corresponding to a vanishing cost. Conversely, if there exists an optimal shape such that $\mathscr{J}(S) = 0$, any such optimum determines a solution of (1)-(4).

Following Tiihonen [28], we need to derive the first and second order shape derivatives for the cost functional $\mathscr{J}(S)$ in (12)-(15) and take leading order terms at the solution of (1)-(4). For this purpose, one needs to first compute the derivative of the state equation (13)-(15) with respect to Ω. According to [27], the shape derivative y' of the solution of problem (13)-(15) with respect to S in the direction $\mathbf{V} \in \mathscr{H}$ satisfies

$$-\Delta y' = 0 \quad \text{in} \quad S, \tag{16}$$

$$y' = 0 \quad \text{on} \quad \Sigma, \tag{17}$$

$$\partial_{\mathbf{n}} y' = \text{div}_{\Gamma}(\nabla_{\Gamma} y \mathbf{V}\cdot\mathbf{n}) + (\frac{\partial \mu}{\partial \mathbf{n}} + \kappa\mu)\mathbf{V}\cdot\mathbf{n} \quad \text{on} \quad \Gamma, \tag{18}$$

where div_{Γ} and ∇_{Γ} stand for the tangential divergence and gradient, respectively, and κ is the mean curvature of Γ.

Lemma 2.1. *Let* Γ *be the free boundary in* (13)-(15)*. Then the shape derivative* y' *of the solution of* (13)-(15) *vanishes.*

Proof. At the solution of the free boundary problem (when $y = 0$ on Σ), we have that $\nabla_{\Gamma} y = 0$ and hence the first term on the right hand side of (18) vanishes. If we exploit the decomposition of Δy

$$\Delta y = \Delta_{\Gamma} y + \frac{\partial^2 y}{\partial \mathbf{n}^2} + \kappa \frac{\partial y}{\partial \mathbf{n}}, \tag{19}$$

where Δ_{Γ} is the Laplace-Beltrami operator on Γ and observe that $\Delta_{\Gamma} y = 0$ since $y = 0$, we get

$$\frac{\partial^2 y}{\partial \mathbf{n}^2} = -\kappa \frac{\partial y}{\partial \mathbf{n}}.$$

Since $\frac{\partial y}{\partial \mathbf{n}} = \mu(\mathbf{x})$ on Γ, we have that

$$\frac{\partial^2 y}{\partial \mathbf{n}^2} = \frac{\partial \mu}{\partial \mathbf{n}} = -\kappa\mu(\mathbf{x}) \quad \text{on} \quad \Gamma.$$

Consequently, the second term on the right hand side of (18) vanishes and the solution to (16)-(18) is $y' = 0$ at the solution of the free boundary problem. □

Proposition 2.1. *If (y,Γ) is a solution of the free boundary problem , then the leading order terms of the shape derivative and Hessian of $\mathscr{J}(S)$ at the solution of* (1)-(4) *is equal to*

$$d\mathscr{J}(S,\mathbf{V}) = \int_\Gamma y\mu\mathbf{V}\cdot\mathbf{n}\, ds,$$

$$d^2\mathscr{J}(S;\mathbf{V},\mathbf{W}) = \int_\Gamma \mu^2\mathbf{W}\cdot\mathbf{n}\mathbf{V}\cdot\mathbf{n}\, ds.$$

Proof. This result follows from Lemma 2.1 and arguments in [28]. □

For an approximate optimal Newton update of Γ, one needs to find a direction $\mathbf{W}$ that solves

$$\int_\Gamma \mu^2\mathbf{W}\cdot\mathbf{n}\mathbf{V}\cdot\mathbf{n}\, ds = -\int_\Gamma y\mu\mathbf{V}\cdot\mathbf{n}\, ds \quad \text{for all } \mathbf{V}\in\mathscr{H}. \tag{20}$$

From (20), we find that $\mathbf{W}(\mathbf{x}) = -\frac{y(\mathbf{x})}{\mu(\mathbf{x})}\mathbf{n}(\mathbf{x})$, and the update of Γ at the k-th step is given by

$$\mathbf{x}^{(k+1)} = \mathbf{x}^{(k)} - \frac{y(\mathbf{x}^{(k)})}{\mu(\mathbf{x}^{(k)})}\mathbf{n}_\varepsilon(\mathbf{x}^{(k)}),$$

where $\mathbf{x}^{(k)} := (x_1^{(k)}, x_2^{(k)}) \in \Gamma^{(k)}$ and $\mathbf{n}_\varepsilon \in H^1(\Gamma)$ is the smoothed normal vector field on the free boundary Γ satisfying

$$\int_\Gamma \varepsilon\nabla_\Gamma\mathbf{n}_\varepsilon\nabla_\Gamma\varphi + \mathbf{n}_\varepsilon\varphi\, ds = \int_\Gamma \mathbf{n}\varphi\, ds, \text{ for all } \varphi\in H^1(\Gamma), \tag{21}$$

with ε some fixed small parameter.

The algorithm to update the free boundary Γ at the k^{th} step now becomes

Algorithm 1 Fixed point algorithm

1: Choose $\Gamma^{(0)}$. Set $j = 0$.
2: Solve the boundary value problem (13)-(15) in $\Omega^{(j)}$.
3: Set $\mathbf{x}^{(j+1)} = \mathbf{x}^{(j)} - \frac{y(\mathbf{x}^{(j)})}{\mu(\mathbf{x}^{(j)})}\mathbf{n}_\varepsilon(\mathbf{x}^{(j)})$, where $\mathbf{x}^{(j)} = (x_1^{(j)}, x_2^{(j)}) \in \Gamma^{(j)}$.
4: If $y^{(j+1)}|_\Gamma$ is small enough, then stop. Otherwise set $j = j+1$ and go to 2.

Following Flucher and Rumpf [11], it can be shown that Algorithm 1 converges with a rate of order 3/2. The less than expected convergence rate is due to the smoothing procedure.

Remark 2.1.

1. The computational domain Ω^j is step 2 of Algorithm 1 is discretized by triangular elements generated by the bi-dimensional anisotropic mesh generator [14]. The boundary value problem (13)-(15) is then discretized using the Galerkin finite-element method. We use polynomials of degree one for the approximation of y. This results in a set of linear algebraic equations that may be represented in matrix form as

$$\mathbf{K}\bar{\mathbf{y}} = \mathbf{F}, \tag{22}$$

where $\mathbf{K}$ is the global system matrix, $\bar{\mathbf{y}}$ is the global vector of unknowns (potential), and $\mathbf{F}$ is a vector that includes the effects of boundary conditions. This linear system is solved by a multi-frontal Gauss LU factorization implemented in the package UMFPACK [8].

2. The coordinates $(x_1, x_2)^T$ in step 3 of Algorithm 1 are defined locally on the free boundary Γ. If we do not provide for the interior node movements, then mesh distortions occur. To avoid this scenario, the following Poisson problem is solved to obtain the interior and boundary vertex displacements,

$$\Delta\Theta = 0, \text{ in } \Omega,$$
$$\Theta = 0, \text{ on } \Sigma, \quad \Theta = -\frac{y(\mathbf{x})}{\mu(\mathbf{x})}\mathbf{n}_\varepsilon(x), \text{ on } \Gamma.$$

Mesh nodes on Σ are fixed, while on Γ, they move in the direction given by the vector field $\mathbf{W}$. The mesh update at the k^{th} time step is now given by

$$(x_1^{j+1}, x_2^{j+1})^T = (x_1^j, x_2^j)^T + \Delta t\ \Theta^j, \tag{23}$$

where $(x_1,\ x_2)$ in (23) are global node locations and Δt is a step size, which must be chosen small to ensure stability of the algorithm [32].

3. Optimization problem

Our control objective consists in determining a control μ such that $\Gamma(\mu)$ is as close as possible to the boundary ∂E of a target Lipschitz domain E such that $\omega \subset E$. The geometric setup of the problem is depicted in Figure 2. According to Theorem 2.1, the solution (y, Ω) of (1)-(4) depends continuously on μ. To emphasize this dependence, we denote this solution by $(y(\mu), \Omega(\mu))$. The boundary $\partial S(\mu)$ of $S(\mu) := \Omega(\mu) \setminus \bar{\omega}$ is a disjoint union of the fixed boundary Σ and the free boundary $\Gamma(\mu)$.

Mathematically, this problem can be expressed as an optimal control problem

$$\begin{cases} \min J((y,\Omega),\mu) \text{ over } ((y,\Omega),\mu) \in W \times U_{ad} \\ \text{subject to } e((y,\Omega),\mu) = 0, \end{cases} \tag{24}$$

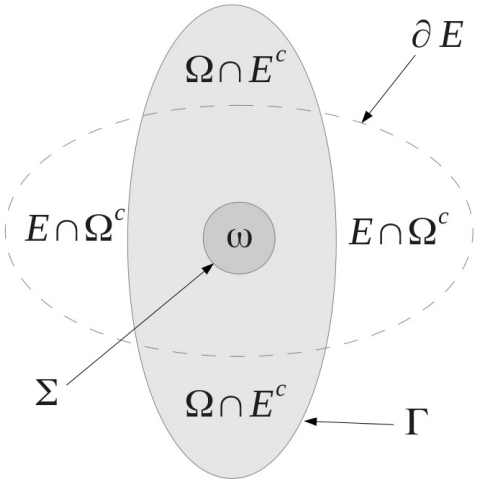

FIGURE 2. "Free" set Ω and target E

where $W := H^1(S) \times \mathcal{O}_{ad}$, $(y,\Omega) \in W$ are the state variables, $\mu \in U_{ad} \subset H^1(\Gamma)$ is the control variable and $e((y,\Omega),\mu) = 0$ is the constraint equation given by (1)-(4). The cost functional J is of tracking type and is given by

$$J((y,\Omega),\mu) = \frac{1}{2}\int_{\Omega\cap E^c} y^2\,dx + \frac{1}{2}\int_{E\cap\omega^c}(y-y_l)^2\,dx + \frac{\beta}{2}\int_\Gamma(\mu^2 + |\nabla_\Gamma \mu|^2)\,ds, \tag{25}$$

where β is the weight of the cost of the control, ∇_Γ denotes the gradient in the direction tangential to the boundary Γ, $y \in H_0^1(\mathcal{D})$ is the extension by zero to $\mathcal{D}$ of the solution of (1)-(4). Further, the target function y_l is chosen as the solution to the linear problem

$$-\Delta y_l = 0 \quad \text{in } E \setminus \overline{\omega}, \tag{26}$$

$$y_l = 1 \quad \text{on } \Sigma, \tag{27}$$

$$y_l = 0 \quad \text{on } \partial E, \tag{28}$$

and is also extended by zero to a function in $H_0^1(\mathcal{D})$. Here, $\mathcal{D}$ denotes an hold- all domain that contains all admissible domains Ω. Extensions of y and y_l by zero to respective elements in $H_0^1(\mathcal{D})$ exist as soon as $\Omega \subset \mathcal{D}$ is measurable, $y = 0$ on $\partial\Omega$, and $y_l = 0$ on ∂E, see [15].

Remark 3.1. *Note that if $\Omega = E$ almost everywhere, then $\Omega \cap E^c = \emptyset$, $u = u_l$ a.e on $E \cap \omega^c$ and thus $J((y,\Omega),0) = 0$. Conversely, if $J((y,\Omega),0) = 0$, then $\Omega = E$ almost everywhere. A contradiction argument is used to support the latter assertion, see,* [20] *for more details.*

The set of admissible controls is the closed convex subset of $H^1(\Gamma)$ given by

$$U_{ad} = \left\{\mu \in H^1(\Gamma) \mid \mu_a \le \mu(\mathbf{x}) \le \mu_b < 0 \text{ a.e. in } \Gamma\right\}. \tag{29}$$

The following theorem establishes the existence of a solution to problem (24).

Theorem 3.1. *There exist an optimal control $\mu_* \in U_{ad}$ minimizing the cost functional in (25) with the optimal state $(y_*, \Omega_*) = (y(\mu_*), \Omega(\mu_*)) \in W$ solving the free boundary problem* (1)-(4).

Proof. Denote the feasible set by

$$\mathscr{F}_{ad} := \{((y,\Omega),\mu) \in W \times H^1(\Gamma) : ((y,\Omega),\mu) \in W \times U_{ad}, \;\; e((y,\Omega),\mu) = 0\}.$$

According to Theorem 2.1, $\mathscr{F}_{ad}$ is nonempty and since since $J \geq 0$, the infimum

$$J_* = \inf_{((y,\Omega),\mu) \in \mathscr{F}_{ad}} J((y,\Omega),\mu)$$

exists and hence we find a minimizing sequence $((y_k,\Omega_k),\mu_k) \subset \mathscr{F}_{ad}$ with

$$\lim_{k\to 0} J((y_k,\Omega_k),\mu_k) = J_*$$

Since $\beta > 0$ and $J((y_k,\Omega_k),\mu_k) \geq \frac{\beta}{2}||\mu_k||_{H^1(\Gamma)}$, the sequence μ_k is bounded. Consequently, we can extract a subsequence again denoted by the same index such that

$$\mu_k \rightharpoonup \mu_* \text{ in } H^1(\Gamma). \tag{30}$$

The limit function μ_* in (30) is an optimal control candidate. According to Theorem 2.1, the state sequences $\{y_k\}, \{\Omega_k\}$ are also bounded in $H_0^1(\mathscr{D})$ and $\mathscr{O}_{ad}$, respectively. Consequently, there exists subsequences, again denoted by the same index such that

$$\tilde{y}_k \rightharpoonup \tilde{y}_* \text{ in } H_0^1(\mathscr{D}), \quad \Gamma_k := \partial\Omega_k \xrightarrow{\Delta} \Gamma_* := \partial\Omega_*, \tag{31}$$

where " ˜ " stands for the zero extension of functions from the domain of their definition on $\mathscr{D}$ and "$\xrightarrow{\Delta}$" for the convergence of boundaries of the sets Ω in the metric defined in (8), [1]. The limit pair (y_*,Ω_*) is the state corresponding to the control μ_*. This results from replacing (y,Ω) with (y_k,Ω_k) in the variational formulation (6)-(7), and taking the limit of the extension of (y_k,Ω_k) onto the domain $\mathscr{D}$, (see, e.g., [13] for more details). Further, it follows from (31) that $\tilde{y}_k \to \tilde{y}_*$ in $L^2(\mathscr{D})$. Consequently, the continuity of J, easily follows, i.e.,

$$J_* = \lim_{k\to\infty} J((y_k,\Omega_k),\mu_k) = J((y_*,\Omega_*),\mu_*).$$

Therefore, $((y_*,\Omega_*),\mu_*)$ is the optimal solution of (24). □

4. Sensitivity analysis

To derive the necessary conditions, we need to differentiate the objective functional $J((y,\Omega),\mu)$ with respect to the control μ, i.e., differentiate the map $\mu \mapsto J((y,\Omega),\mu)$. To achieve this, the derivative of the map $\mu \mapsto (y(\mu),\Omega(\mu))$ is needed.

4.1. **Sensitivity of (y,Ω) with respect to μ.** Starting from the solution (Ω, y) of (1)-(4), consider a solution of the perturbed problem

$$\begin{cases} -\Delta y^\varepsilon = 0 \quad \text{in} \quad S^\varepsilon, \\ y^\varepsilon = 1 \quad \text{on} \quad \Sigma \\ y^\varepsilon = 0 \quad \text{on} \quad \Gamma^\varepsilon, \\ \partial_{\mathbf{n}} y^\varepsilon = \mu + \varepsilon\delta\mu \quad \text{on} \quad \Gamma^\varepsilon, \end{cases} \tag{32}$$

with a smooth function $\delta\mu$ defined on Γ. Following [11], we assume that in the limit $\varepsilon \to 0$, the solution can be expanded as

$$\Gamma^\varepsilon = \Gamma + \varepsilon\mathbf{V} + O(\varepsilon^2), \tag{33}$$

$$y^\varepsilon = y + \varepsilon y' + O(\varepsilon^2), \tag{34}$$

with a smooth function y' defined on S, $\mathbf{V} = v_n\mathbf{n}$ where $\mathbf{n}$ is the normal vector to Γ and v_n is some scalar valued function on Γ. In this sense, $(\mathbf{V}, y')$ is the classical first variation of (Ω, y) with respect to variation $\delta\mu$ of the Neumann data μ on Γ.

Theorem 4.1. *The first variation y' of a solution $y : S \mapsto \mathbb{R}$ of the Bernoulli's free boundary problem subject to a variation $\delta\mu$ of the Neumann data on Γ is given by the solution to the linearized problem*

$$\begin{cases} -\Delta y' = 0 \quad \textit{in} \quad S, \\ y' = 0 \quad \textit{on} \quad \Sigma, \\ \partial_{\mathbf{n}} y' + \kappa y' = \delta\mu \quad \textit{on} \quad \Gamma, \end{cases} \tag{35}$$

where κ is the mean curvature of Γ and

$$v_n = -\frac{y'}{\mu}, \quad \textit{on } \Gamma. \tag{36}$$

Proof. Following [11], we expand the unperturbed potential and its normal derivative at the free boundary:

$$y(\mathbf{x} + \varepsilon\mathbf{V}) = \varepsilon\mu v_n + O(\varepsilon^2), \tag{37}$$

$$\frac{\partial y}{\partial \mathbf{n}}(\mathbf{x} + \varepsilon\mathbf{V}) = \mu + \varepsilon\frac{\partial^2 y}{\partial \mathbf{n}^2}(\mathbf{x})v_n + O(\varepsilon^2). \tag{38}$$

Since $\Delta y = \Delta_\Gamma y + \frac{\partial^2 y}{\partial \mathbf{n}^2} + \kappa\frac{\partial y}{\partial \mathbf{n}}$, and $\Delta y = \Delta_\Gamma y = 0$, we have that $\frac{\partial^2 y}{\partial \mathbf{n}^2} = -\kappa\frac{\partial y}{\partial \mathbf{n}}$. Hence, the second equation in (38) can be expressed as

$$\begin{aligned} \frac{\partial y}{\partial \mathbf{n}}(\mathbf{x} + \varepsilon\mathbf{V}) &= \mu - \varepsilon\kappa\mu v_n + O(\varepsilon^2) \\ &= \mu - \kappa y(\mathbf{x} + \varepsilon\mathbf{V}) + O(\varepsilon^2). \end{aligned} \tag{39}$$

Utilizing (34), we can expand the Neumann condition for the perturbed problem as

$$\frac{\partial y^\varepsilon}{\partial \mathbf{n}}(\mathbf{x}+\varepsilon\mathbf{V}) = \frac{\partial y}{\partial \mathbf{n}}(\mathbf{x}+\varepsilon\mathbf{V}) + \varepsilon\frac{\partial y'}{\partial \mathbf{n}}(\mathbf{x}+\varepsilon\mathbf{V}). \tag{40}$$

Using (39), the right hand side of (40) can be expressed as

$$\frac{\partial y^\varepsilon}{\partial \mathbf{n}}(\mathbf{x}+\varepsilon\mathbf{V}) = \mu - \kappa y(\mathbf{x}+\varepsilon\mathbf{V}) + \varepsilon\frac{\partial y'}{\partial \mathbf{n}}(\mathbf{x}+\varepsilon\mathbf{V}). \tag{41}$$

Using the last equation in (32), we find

$$\mu + \varepsilon\delta\mu = \mu - \kappa y(\mathbf{x}+\varepsilon\mathbf{V}) + \varepsilon\frac{\partial y'}{\partial \mathbf{n}}. \tag{42}$$

Note that

$$0 = y^\varepsilon(\mathbf{x}+\varepsilon\mathbf{V}) = y(\mathbf{x}+\varepsilon\mathbf{V}) + \varepsilon y'(\mathbf{x}+\varepsilon\mathbf{V}). \tag{43}$$

Utilizing (43) in (42), we obtain

$$\frac{\partial y'}{\partial \mathbf{n}}(\mathbf{x}+\varepsilon\mathbf{V}) + \kappa y'(\mathbf{x}+\varepsilon\mathbf{V}) = \delta\mu + O(\varepsilon).$$

In the limit as ε tends to zero, we recover the second boundary condition in (32). Observe that from (38) and (43), we obtain the expression for v_n. □

4.2. **Sensitivity of J with respect to μ.**

Lemma 4.1. *Let us assume that $\partial_{\mathbf{n}}\mu = 0$ on $\partial\Gamma$, where $\partial\Gamma$ denotes a boundary of Γ viewed as a subset of Γ. Then the directional derivative of the cost J with respect to $\mu \in H^1(\Gamma)$ in the direction $\delta\mu \in H^1(\Gamma)$ is given by*

$$J'_\mu\delta\mu = \int_\Gamma (p + \beta\mu - \beta\Delta_\Gamma\mu)\delta\mu \, ds, \tag{44}$$

where Δ_Γ denotes the Laplace operator along the boundary Γ, and p is the adjoint state satisfying

$$-\Delta p = y\mathbb{1}_{\Omega(\mu)\cap E^c} + (y - y_l)\mathbb{1}_{E\cap\omega^c} \quad in \quad S, \tag{45}$$

$$p = 0 \quad on \quad \Sigma, \tag{46}$$

$$\partial_{\mathbf{n}}p + \kappa p = 0 \quad on \quad \Gamma. \tag{47}$$

Proof. Since J is quadratic and the fact that (y,Ω) is differentiable with respect to μ, we infer that the direction derivative of J with respect to μ exist and is given by

$$J'_\mu\delta\mu = \int_{\Omega\cap E^c} yy' \, dx + \int_{E\cap\omega^c} (y - y_l)y' \, dx + \beta\int_\Gamma \mu\delta\mu + \nabla_\Gamma\mu\nabla_\Gamma\delta\mu \, ds. \tag{48}$$

Since $\partial_{\mathbf{n}}\mu = 0$ on $\partial\Gamma$, integrating by parts to remove derivatives from $\delta\mu$, one obtains

$$J'_\mu\delta\mu = \int_{\Omega\cap E^c} yy' \, dx + \int_{E\cap\omega^c} (y - y_l)y' \, dx + \beta\int_\Gamma (\mu - \Delta_\Gamma\mu)\delta\mu \, ds. \tag{49}$$

Multiplying the sensitivity equation (35) with the adjoint state p and applying Greens formula, we find

$$\int_S (y\mathbb{1}_{\Omega(\mu)\cap E^c} + (y-y_l)\mathbb{1}_{E\cap\omega^c})y'\,dx = \int_\Gamma p\,\partial_n y' - y'\,\partial_n p\,ds. \tag{50}$$

Utilizing the boundary conditions in (47) and (35), we can express the right hand side in (50) as

$$\int_S (y\mathbb{1}_{\Omega(\mu)\cap E^c} + (y-y_l)\mathbb{1}_{E\cap\omega^c})y'\,dx = \int_\Gamma p\delta\mu\,ds. \tag{51}$$

Combining (51) and (49), gives the desired result. □

If we restrict the control μ in the above Lemma to belong to a convex set U_{ad} of admissible controls, then the following result furnishes the first order optimality condition.

Corollary 4.1. *Let $\delta\mu := (\mu-\mu_*)$ where $\mu_* \in U_{ad}$ denotes an optimal control given by Theorem 3.1. Then the first order optimality condition satisfied by μ_* is*

$$J'_{\mu_*}\delta\mu = \int_\Gamma (p^* + \beta(\mu_* - \Delta_\Gamma\mu_*))\delta\mu\,ds \geq 0, \text{ for all } \mu\in U_{ad}, \tag{52}$$

where p^* is the unique solution to the adjoint state (45)-(47).

Proof. The proof can be constructed following arguments in [31]. □

5. Numerical algorithm and examples

We solve the optimization problems using an iterative process, i.e., we find a solution to the lower-level problem (1)-(4) first and then proceed to the upper-level problem consisting of the minimization of J. For the upper-level problem, we use a gradient method with projection. If we denote the projection of an element $\tilde{\mu}\in L^2(\Gamma)$ onto the convex set U_{ad} by $P_{U_{ad}}\tilde{\mu}$, then $P_{U_{ad}}\tilde{\mu}$ is characterized by

$$(\tilde{\mu} - P_{U_{ad}}\tilde{\mu}, \mu - P_{U_{ad}}\tilde{\mu})_{L^2(\Gamma)} \leq 0 \quad \text{for all } \mu\in U_{ad}. \tag{53}$$

The optimality condition in (52) is equivalent to

$$(\mu_* - \rho J'_{\mu_*}\delta\mu - \mu_*, \mu-\mu_*)_{L^2(\Gamma)} \leq 0 \quad \text{for all } \mu\in U_{ad}, \tag{54}$$

where ρ is any positive number. It can be verified, see, e.g., [16] that this variational inequality is equivalent to

$$\mu_* = P_{U_{ad}}(\mu_* - \rho J'_{\mu_*}), \tag{55}$$

where $J'_{\mu_*} = p^* + \beta\mu_* - \beta\Delta_\Gamma\mu_* \in L^2(\Gamma)$. Thus, μ_* is a fixed point of the mapping Φ_ρ defined by

$$\Phi_\rho(\mu) = P_{U_{ad}}(\mu - \rho J'_\mu). \tag{56}$$

The gradient method with projection consists in calculating a fixed point of Φ_ρ. The steps for computing this fixed point are outlined in Algorithm 2.

Algorithm 2 Bilevel optimization algorithm

1: Choose initial shape Ω_0, tol, N_{max}, $\mu_0 \in U_{ad}$;
2: **while** ($(err > tol)$ & $(k < N_{max})$) **do**
3: Solve (1)-(4) using Algorithm 1 with $\mu = \mu^k$.
4: Compute the adjoint system (45)-(47).
5: Evaluate the descent direction $\delta\mu$ with $\delta\mu = -(p + \beta\mu_k) + \beta\Delta_\Gamma\mu_k$.
6: Compute $\rho_k \in (0,1]$ such that

$$J((y,\Omega_k),\mu_k + \rho_k\delta\mu) = \min\{J((y,\Omega_k),P_{U_{ad}}(\mu_k + \rho\delta\mu)) \ : \ \rho \in (0,1]\}.$$

7: Set $\mu^{k+1} = P_{U_{ad}}(\mu_k + \rho_k\delta\mu)$
8: Set $err_k = ||\mu^{k+1} - \mu^k||_{H^1(\Gamma)}$.
9: **end while**

Remark 5.1. *The evaluation of the descent direction $\delta\mu$ in step 5 of Algorithm 2 amounts to solving the PDE*

$$\int_\Gamma \delta\mu\varphi + \int_\Gamma \beta\nabla_\Gamma\mu\nabla_\Gamma\varphi + (p + \beta\mu)\varphi \, ds = 0, \text{ for all } \ \varphi \in H^1(\Gamma). \tag{57}$$

Furthermore, the projection $P_{U_{ad}}$ in steps 6 and 7 of Algorithm 2 ensures that the computed controls are admissible. It is defined as

$$P_{U_{ad}}(\mu) = \min\{\mu_b, \max\{\mu_a, \mu\}\}.$$

Moreover, the line search procedure in step 6 is not implemented exactly. Rather, we utilize the Armijo-rule with backtracking to determine an approximation of ρ_k.

5.1. **Example 1.** We start with the case where the optimal μ is known. Our goal is then to reconstruct the value of μ. For this purpose, we solve the free boundary problem (1)-(4) with the value of μ set to $\mu = -10$. The boundary $\Sigma := \partial\omega$ is chosen as the boundary of the T-shape

$$\omega := ((-3/8, 3/8) \times (-1/4, 0)) \cup ((-1/8.1/8) \times (0, 1/4)) \subset \mathbb{R}^2. \tag{58}$$

Algorithm 1 is utilized to determine the location of the free boundary. As an initial guess Γ_0 for this algorithm, a circle of radius 0.75 is chosen. We run Algorithm 1 until $||y||_{L^2(\Gamma)} < 10^{-5}$. This stopping criterion is met after 8 iterations and the resulting geometry solving the free boundary problem is depicted in Figure 3.

The domain in Figure 3 is now chosen as the target domain (E) for the optimization Algorithm 2. To determine the corresponding objective function y_l in the cost J in (25), the PDE in (26)-(28) is solved on this target domain. The following parameters are chosen for the initialization of Algorithm 2. The control μ is initialized with the value $\mu_0 = -1$ defined

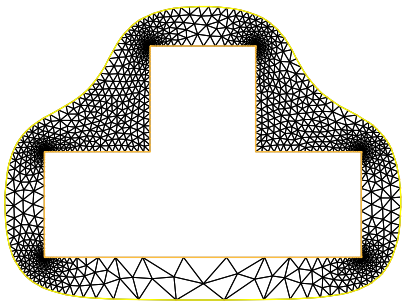

FIGURE 3. Target domain

over the entire initial domain $S_0 = \Omega_0 \setminus \bar{\omega}$. The interior boundary $\Sigma := \partial\omega$ of S_0 is chosen as the boundary of the T-shape (58) and outer boundary Γ, a circle of radius 0.75. The value of β is set to $\beta = 10^{-5}$, and the lower and upper values of the control constraint (μ_a, μ_b) are set to $\mu_a = -15$ and $\mu_b = -0.01$. The maximum number of iteration count (N_{max}) is set to 500 and the value of tol to 10^{-5}. We run Algorithm 2 until $||\delta\mu||_{H^1(\Gamma)} < tol$. This stopping criterion is met after 128 iterations with the final value of the cost of magnitude 1.97×10^{-7}.

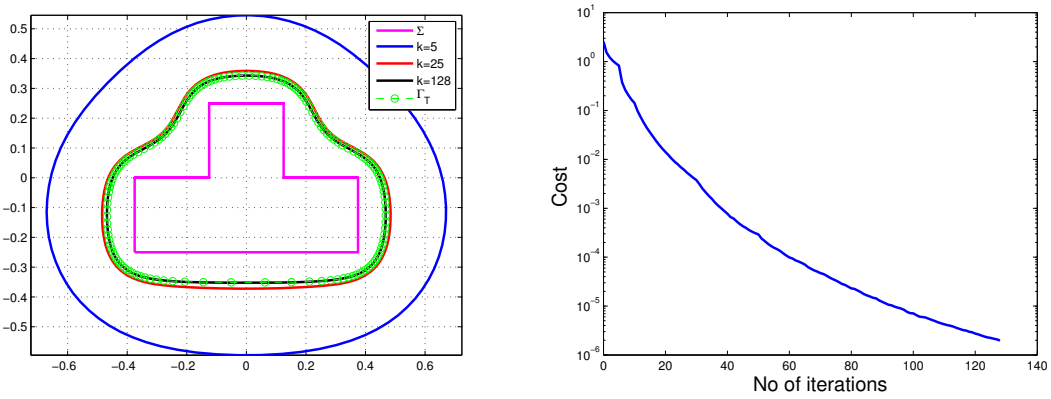

(a) Histories of outer boundaries (b) History of cost

FIGURE 4. Histories of outer boundaries and cost

The histories of domains and of the cost (in a semi-logarithmic scale) are depicted in Figure 4. From Figure 4(a), we observe that as the iteration count increases, the outer boundary Γ converge to the target boundary ∂E. Furthermore, as the iteration count increases, the value of the cost J decreases as expected. Moreover, it is also observed that the number of iterations (j) required for the convergence of the inner Algorithm 1 reduce to $j = 0$ as Γ approaches ∂E. This is the case since $\delta\mu \to 0$ in $H^1(\Gamma)$ as $\Gamma \xrightarrow{\Delta} \partial E$, for β sufficiently small. In Figure 5(a) and 5(b), the distribution of the optimal control $\mu_*(x_1, x_2)$ arising from

optimization and its variation with respect to x_2 on Γ for $x_1 \leq 0$ are depicted. From Figure 5(a), we observe that the optimal value of μ is approximately $\mu_* \approx -10$ on Γ as expected. On Σ, there is no variation in μ since $p = 0$ and β is small and hence $\mu_* \approx \mu_0 = -1$. From

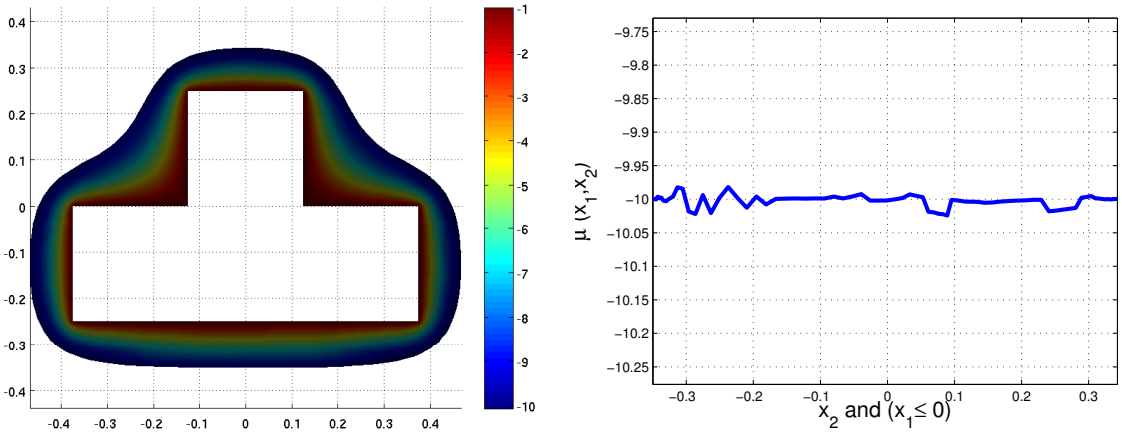

(a) Distribution of μ.

(b) Restriction of μ to Γ for $x_1 \leq 0$

FIGURE 5. Optimal control μ

Figure 5(b), we observe that μ_* on Γ in the region $x_1 \leq 0$, actually varies between -10.0242 to -9.9819 with a mean variation $\overline{\mu_*} = -10.0018$. The slight deviation of ± 0.02 from the expected value ($\mu = -10$) arises from the discretization error.

5.1.1. *Role of β.* It is obvious that the results above can be altered if we chose a different value of the regularization parameter β. By varying the value of β, the balance between the two terms $J_1 := \frac{1}{2}\int_{\Omega\cap E^c} y^2 \, dx + \frac{1}{2}\int_{E\cap\omega^c}(y - y_l)^2 \, dx$ and $J_2 := \frac{\beta}{2}\int_\Gamma \mu^2 + |\nabla_\Gamma \mu|^2 \, ds$ in the cost functional J will be altered. For this purpose, we solve the optimal control problem (24) for varying parameters $\beta \in \{10^{-5}, 10^{-2}, 5\times 10^{-2}\}$. Other parameters for the initialization of Algorithm 2 are set as before and are fixed for each β. For each $\beta \in \{10^{-5}, 10^{-2}, 5\times 10^{-2}\}$, Algorithm 2 is run until $||\delta\mu||_{H^1(\Gamma)} < 10^{-5}$. This stopping criterion is met after 128, 70 and 20 iterations, for $\beta = 10^{-5}, 10^{-2}$ and 5×10^{-2}, respectively, with the corresponding final values of the cost of magnitude 1.97×10^{-7}, 0.23, and 0.74. The optimal outer boundaries corresponding to each $\beta \in \{10^{-5}, 10^{-2}, 5\times 10^{-2}\}$ are depicted in Figure 6. From Figure 6, we see that for large values of β, the optimization problem is easy to solve (less number of iterations) but Ω does match E. On the other hand, if β is chosen small, then the optimization problem is harder to solve but Ω matches E closely.

Therefore, if it is extremely important for J_1 to be very small but we are less concerned by the size of J_2 , then a small value of β should be chosen. Conversely, if Ω does not need to closely match E but it is important that J_2 remains small, then a larger value of β would be used. Since the former is our concern, we shall chose β small in the following examples.

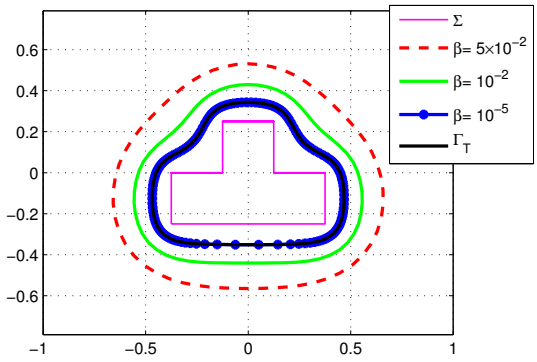

FIGURE 6. Optimal domains for varying regularizations β

5.2. **Example 2.** In this example, we choose a target domain E with a smooth boundary ∂E. Our goal is to find an optimal control μ such that the free boundary Γ, a solution to (1)-(4) is as close as possible to ∂E in the sense of cost functional J. The fixed boundary $\Sigma := \partial\omega$ is chosen as in (58), and the target boundary ∂E as that of an ellipse given by

$$E := \left\{(x,y) \in \mathbb{R}^2 \ : \ \frac{x^2}{0.95^2} + \frac{y^2}{0.65^2} = 1\right\}. \tag{59}$$

We initialize Algorithm 2 with the domain $\Omega^0 \setminus \omega$, where

$$\Omega^0 := \left\{(x,y) \in \mathbb{R}^2 \ : \ x^2 + y^2 = 0.75^2\right\}.$$

The initial and target shapes, are depicted in Figure 7(a). We set the initial value of $\mu_0 = -1$.

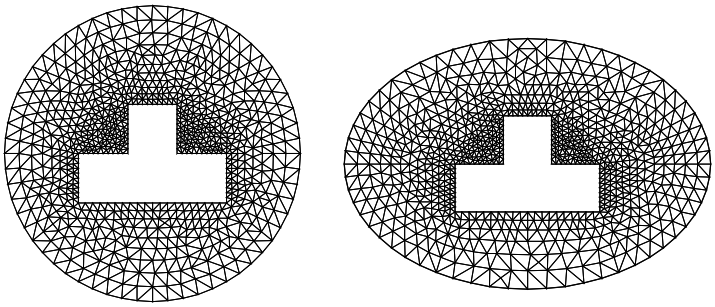

(a) Initial domain (b) Target domain

FIGURE 7. Initial and target domains

The value of β and the parameters in U_{ad} are set as in the previous example. We run Algorithm 2 until $||\delta\mu||_{H^1(\Gamma)} < 10^{-5}$. This stopping criterion is met after 54 iterations with the final value of the cost of magnitude 4.27×10^{-6}. The convergence history of the outer

boundaries is depicted in Figure 8(a). It is observed that as the iteration count increases, the outer boundaries converge to the target ∂E. In Figure 8(b), the optimal control is depicted. As expected, more control is applied on sections of the boundary Γ with large curvature.

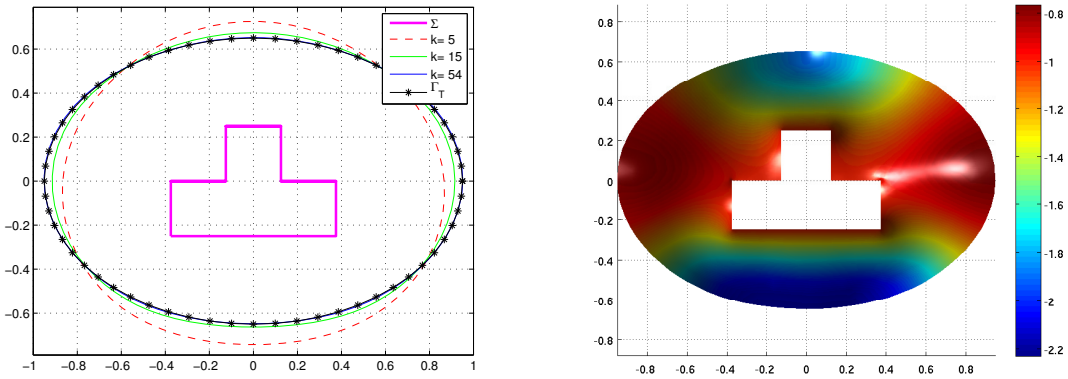

(a) Histories of outer boundaries (b) Optimal control

FIGURE 8. History of outer boundaries and optimal control

5.3. **Example 3.** In this example our aim is to check whether there exists a control $\mu \in \mathscr{U}_{ad}$ such that the optimal boundary Γ_* is as close as possible to a target ∂E which is not of class $\mathscr{C}^{1,1}$. The cost functional J is minimized with the boundary ∂E of the target domain E represented by the parametric equations

$$
\begin{aligned}
x(t) &= 0.7 + 0.75\cos(2\pi t)(1-\cos(2\pi t)), \quad t \in (0,1),\\
y(t) &= -0.1 + 0.75\sin(2\pi t)(1-\cos(2\pi t)), \quad t \in (0,1).
\end{aligned} \tag{60}
$$

It is clear from the parameterization in (60), that the target is not of class $\mathscr{C}^{1,1}$. We initialize Algorithm 2 with the domain $\Omega^0 \setminus \omega$, where $\Omega^0 := \{(x,y) \in \mathbb{R}^2 \ : \ x^2 + y^2 = 0.65^2\}$. The initial and target shapes, are depicted in Figure 9. The control μ is initialized with the value $\mu_0 = -1$ defined over the entire initial domain $S_0 = \Omega_0 \setminus \bar{\omega}$. The value of β and the parameters in U_{ad} are set as in the previous example. We run Algorithm 2 until $||\delta\mu||_{H^1(\Gamma)} < 10^{-5}$. This stopping criterion is met after 67 iterations with the final value of the cost of magnitude 6.91×10^{-4}.

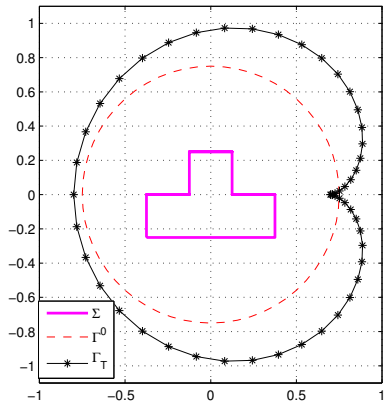

FIGURE 9. Initial and target domains

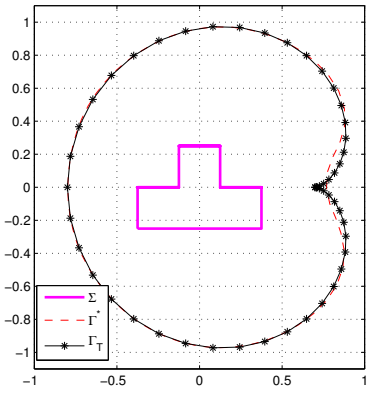

(a) Target and optimal outer boundary

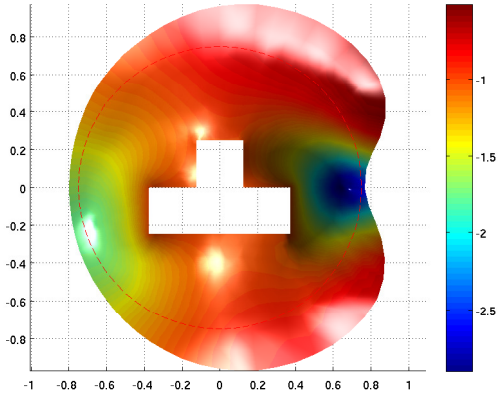

(b) Optimal control

FIGURE 10. History of outer boundaries and optimal control

The target and optimal outer boundary are depicted in Figure 10(a). For the smooth section of the target boundary ∂E, the optimal boundary matches it exactly. For the part of ∂E with cusp, the optimal boundary is smoothed and does not match the target as expected. In Figure 10(b), the distribution of the optimal μ is depicted. As expected, it is clearly seen from Figure 10(b) that more control is applied in regions where the initial boundary Γ_0 is far from the target.

CONCLUSION

In this paper, we have considered an optimal control of a Bernoulli free boundary problem, where the interface is explicitly parametrized using the position of nodes at the interface.

A Neumann flux on the free boundary is utilized as a control parameter and the sensitivity analysis of the resultant optimization problem is performed using the shape perturbation analysis concepts.

A segregation algorithm based on first order gradient information for solving this free boundary PDE constrained optimal control problem has been proposed and implemented. The numerical results presented here indicate that location of the external free boundary can be controlled by changing the Neumann flux on the free boundary. It remains to investigate the usage of second order gradient information to speed up the algorithm for solving this bilevel optimization problem. Furthermore, the extension of the results in this paper to other bilevel optimization problems governed by complicated flow equations like the Navier-Stokes equations with surface tension is also an interesting subject of the future.

REFERENCES

[1] A. Acker and R. Meyer. A free boundary problem for the p-Laplacian: Uniqueness, convexity, and successive approximation of solutions. *Electronic Journal of Differential Equations*, 1995(8):1–20, 1995.

[2] H.W. Alt and L.A. Caffarelli. Existence and regularity for a minimum problem with free boundary. *J. reine angew. Math*, 325:105–144, 1981.

[3] Martin K. Bernauer and Roland Herzog. Optimal control of the classical two-phase Stefan problem in level set formulation. *SIAM J. Sci. Comput.*, 33(1):342–363, February 2011.

[4] F. Bouchon, S. Clain, and R. Touzani. Numerical solution of the free boundary Bernoulli problem using a level set formulation. *Comput. Methods Appl. Mech. Engrg.*, 194(36-38):3934–3948, 2005.

[5] F. Bouchon, S. Clain, and R. Touzani. A perturbation method for the numerical solution of the Bernoulli problem. *J. Comput. Math.*, 26(1):23–36, 2008.

[6] J. Bracken and J.T. McGill. Mathematical programs with optimization problems in the constraints. *Operations Res.*, 21:37–44, 1973. Mathematical programming and its applications.

[7] B. Colson, P. Marcotte, and G. Savard. Bilevel programming: a survey. *4OR*, 3(2):87–107, 2005.

[8] T. A. Davis and I. S. Duff. A combined unifrontal/multifrontal method for unsymmetric sparse matrices. *ACM Trans. Math. Softw.*, 25(1):1–20, 1999.

[9] M. C. Delfour and J. P. Zolésio. *Shapes and geometries: analysis, differential calculus, and optimization*. Society for Industrial and Applied Mathematics, Philadelphia, PA, USA, 2001.

[10] K. Eppler and H. Harbrecht. On a Kohn-Vogelius like formulation of free boundary problems. *Computational Optimization and Applications*, 52(1):69–85, 2012.

[11] M. Flucher and M. Rumpf. Bernoulli's free boundary problem, qualitative theory and numerical approximation. *J. Reine Angew. Math*, 486:165–204, 1997.

[12] J. Haslinger, K. Ito, T. Kozubek, K. Kunisch, and G. Peichl. On the shape derivative for problems of Bernoulli type. *Interfaces and Free Boundaries*, 11(2):317–330, 2009.

[13] J. Haslinger and R. A. E. Mäkinen. *Introduction to Shape Optimization: Theory, Approximation, and Computation*. Society for Industrial and Applied Mathematics, Philadelphia, PA, USA, 2003.

[14] F. Hecht. Bamg: Bidimensional anisotropic mesh generator. `http://www.rocq.inria.fr/gamma/cdrom/www/bamg/eng.html`, 1998.

[15] A. Henrot and M. Pierre. *Variation et Optimisation de Formes, Mathématiques et Applications*. Springer-Verlag, Berlin, 2005.

[16] M. Hinze, R. Pinnau, M. Ulbrich, and S. Ulbrich. *Optimization with PDE constraints*, volume 22 of *Mathematical Modelling: Theory and Applications*. Springer, New York, 2009.

[17] M. Hinze and S. Ziegenbalg. Optimal control of the free boundary in a two-phase Stefan problem. *J. Comput.Phys*, 223:657âĂŞ684, 2007.
[18] M. Hinze and S. Ziegenbalg. Optimal control of the free boundary in a two-phase Stefan problem with flow driven by convection. *Z. Angew. Math. Mech*, 87:430âĂŞ448, 2007.
[19] K. Ito, K. Kunisch, and G. Peichl. Variational approach to shape derivatives for a class of Bernoulli problems. *Journal of Mathematical Analysis and Applications*, 314(1):126–149, 2006.
[20] H. Kasumba, K. Kunisch, and A. Laurain. A bilevel shape optimization problem for the exterior Bernoulli free boundary value problem. *RICAM report*, (16), 2013.
[21] K. Kunisch and K. Ito. *Lagrange multiplier approach to variational problems and applications.*, volume 15 of *Advances in Design and Control*. Society for Industrial and Applied Mathematics (SIAM), Philadelphia, PA, 2008.
[22] A. Laurain and Y. Privat. On a Bernoulli problem with geometric constraints. *ESAIM Control Optim. Calc. Var.*, 18(1):157–180, 2012.
[23] G. Panaras, A. Theodorakakos, and G. Berggeles. Numerical investigation of the free surface in a continuous steel casting mold model. *Metallurgical and Materials Transactions B*, 29:1117–1126, 1998. 10.1007/s11663-998-0081-3.
[24] Bartosz Protas and Wenyuan Liao. Adjoint-based optimization of PDEs in moving domains. *Journal of Computational Physics*, 227(4):2707 – 2723, 2008.
[25] S. Repke, N. Marheineke, and R. Pinnau. Two adjoint-based optimization approaches for a free surface Stokes flow. *SIAM Journal on Applied Mathematics*, 71(6):2168–2184, 2011.
[26] K. Selvanayagam, T. Götz, S. Sundar, and V. Vetrivel. Optimal control of film casting processes. *Int. J. Numer. Meth. Fluids*, 59:1111–1124, 2009.
[27] J. Sokolowski and J. P. Zolésio. *Introduction to Shape Optimization. Shape Sensitivity Analysis*. Springer-Verlag, 1992.
[28] T. Tiihonen. Shape optimization and trial methods for free boundary problems. *Mathematical Modelling and Numerical Analysis*, 31:805–825, 1997.
[29] J. I. Toivanen, J. Haslinger, and R. A. E. Mäkinen. Shape optimization of systems governed by Bernoulli free boundary problems. *Computer Methods in Applied Mechanics and Engineering*, 197(15):3803–3815, 2008.
[30] J. I. Toivanen, J. Haslinger, and R. A. E. Mäkinen. Topology optimization in Bernoulli free boundary problems. *Journal of Engineering Mathematics*, pages 1–16, 2012.
[31] F. Trötzsch. *Optimal control of partial differential equations: Theory methods and applications*. AMS, Providence, 2010.
[32] E. P. VanLohuizen, P. J. Slikkerveer, and S. B. G. O'Brien. An implicit surface tension algorithm for Picard solvers of surface-tension-dominated free and moving boundary problems. *International Journal for Numerical Methods in Fluids*, 22(9):851–65, 1996.
[33] O. Volkov, B. Protas, W. Liao, and D. W. Glander. Adjoint-based optimization of thermo-fluid phenomena in welding processes. *J. Eng. Math*, 65(3):201–220, 2009.

(H. Kasumba) JOHANN RADON INSTITUTE FOR COMPUTATIONAL AND APPLIED MATHEMATICS, AUSTRIAN ACADEMY OF SCIENCES, ALTENBERGERSTRASSE 69, A-4040 LINZ, AUSTRIA
E-mail address: henry.kasumba@oeaw.ac.at